STEM CELLS AND DEVELOPMENT
Volume 20, Number 10, 2011

DOI: 10.1089/scd.2010.0418

The Epigenetic Regulation of Stem Cell Factors in Hepatic Stellate Cells

Sven Reister,* Claus Kordes,* Iris Sawitza,* and Dieter Häussinger

The epigenetic regulation by DNA methylation is an important mechanism to control the expression of stem cell factors as demonstrated in tumor cells. It was recently shown that hepatic stellate cells (HSC) express stem/progenitor cell factors and have a differentiation potential. The aim of this work was to investigate if the expression of stem cell markers is regulated by DNA methylation during activation of rat HSC. It was found that *CD133*, *Notch1*, and *Notch3* are regulated via DNA methylation in HSC, whereas *Nestin* shows no DNA methylation in HSC and other undifferentiated cells such as embryonic stem cells and umbilical cord blood stem cells from rats. In contrast to this, DNA methylation controls *Nestin* expression in differentiated cells like hepatocytes and the hepatoma cell line H4IIE. Demethylation by 5-Aza-2-deoxycytidine was sufficient to induce Nestin in H4IIE cells. In quiescent stellate cells and embryonic stem cells, the *Nestin* expression was suppressed by histone H3 methylation at lysine 9, which is another epigenetic mechanism. Apart from the known induction of Nestin in cultured HSC, this intermediate filament protein was also induced after partial hepatectomy, indicating activation of HSC during liver regeneration. Taken together, this study demonstrates for the first time that the expression of stem cell-associated factors such as CD133, Notch1, and Notch3 is controlled by DNA methylation in HSC. The regulation of *Nestin* by DNA methylation seems to be restricted to differentiated cells, whereas undifferentiated cells use different epigenetic mechanisms such as histone H3 methylation to control *Nestin* expression.

Introduction

Epigenetic gene regulation is essential to maintain a cell-type-specific expression profile. The term epigenetic can be defined as "mitotically and/or meiotically heritable changes in gene function that cannot be explained by changes in DNA sequences" [1]. Mechanisms of gene regulation without changes in the sequence of nucleotides are the DNA methylation, chromatin remodeling via histone modification, and RNA interference [2–4]. The methylation of DNA is performed by specific DNA methyltransferases (Dnmt), which selectively transfer a methyl group to the C5 atom of cytosine at a cytosine phosphatidyl guanosine site (5′-CpG-3′). Cytosine methylation is restricted to this sequence in mammals. There are 2 different mechanisms of DNA methylation, which are mediated by different methyltransferases. The first is called *de novo* DNA methylation, where mainly the enzymes Dnmt3a and Dnmt3b methylate selectively CpG [5]. Another Dnmt methylates CpG dinucleotides during DNA replication [6]. This is realized by the enzyme Dnmt1, which replicates the regulatory modification of the DNA through methylation in mitotic cells [7]. The importance of a proper DNA methylation for embryogenesis is widely accepted, because it was shown that the offspring of mice harboring a knockout for one of the Dnmt genes die early during development [8,9]. Also, maternal and paternal imprinting is mediated by this epigenetic mechanism [10]. Apart from this, it was shown for many tumors that a dysregulation of DNA methylation such as a hypermethylation of the tumor suppressor gene $P16^{ink4a}$ protects the tumor cells from cell cycle arrest [11]. In addition to gene suppression, tumors often express genes that are normally found in stem cells or during early development [12]. In several cancer types, *CD133*, a stem/progenitor cell-associated gene, is expressed after DNA demethylation [13,14].

Epigenetic mechanisms are also very important for the maintenance of stem cells and their differentiation during asymmetric division [15]. Owing to the expression of stem cell factors in hepatic stellate cells (HSC) [16] and the fact that these factors are often regulated by DNA methylation [17], we examined their regulation by epigenetic mechanisms in rat HSCs. Quiescent HSC express glial fibrillary acidic protein (*GFAP*) as well as the stem cell markers *CD133* and *Notch1*, but both factors are repressed after HSC activation in culture [18,19]. On the other hand, culture-activated stellate cells start to express *Nestin* [20], which is a marker of

Klinik für Gastroenterologie, Hepatologie und Infektiologie, Heinrich-Heine-Universität, Düsseldorf, Germany.
*These three authors contributed equally to this work.

activated somatic stem/progenitor cells [21]. To unravel a possible involvement of epigenetic mechanisms in the regulation of gene expression during stellate cell activation, the DNA methylation of genes that are associated with stem cell characteristics was analyzed in the present study. The focus was on DNA methylation studies of *Nestin* and *CD133* to demonstrate that stellate cells of the liver display similarities to established stem/progenitor cells in the regulation of these factors. Since the expression of Nestin by activated HSC of rats is well accepted [20] and specific antibodies are available for this protein, Nestin was also used to monitor the activation of HSC during liver regeneration after partial hepatectomy (PH). In contrast to α-smooth muscle actin (α-SMA), which was often applied to detect activated HSC, Nestin occurs in stem/progenitor cells that maintain their developmental potential. The induction of Nestin was investigated in the PH model in the absence and presence of 2-acetylaminofluorene (AAF). The latter is an established model to suppress hepatocyte proliferation and to induce stem cell-based liver regeneration [22].

First studies exist about the epigenetic regulation of gene expression during activation of HSC with regard to fibrogenesis [23,24]. However, there is growing evidence that the activation of stellate cells is not restricted to the appearance of fibrosis [25], but rather represents the onset of a developmental process that involves a switch of Notch1 to Notch3 receptor. Notch1 is essential to maintain stem cells in their niche [19,26], whereas Notch3 is apparently involved in further development of stem/progenitor cells [27]. For this reason, the DNA methylation of these Notch receptors was also analyzed in the present study.

Materials and Methods

Cells and cell culture

Stellate cells were isolated from the liver of male Wistar rats (500–600 g body mass) by an enzymatic perfusion (Collagenase H Roche; Pronase E, Merck) and enriched by density gradient centrifugation as described [28]. Collected stellate cells were cultured in Dulbecco's modified Eagle's medium (DMEM) containing 10% fetal calf serum (FCS Gold; PAA Laboratories) and 1% antibiotic/antimycotic solution (100×; Gibco, Invitrogen). Hepatocytes were isolated by collagenase CLS type II (Biochrom) perfusion of the liver and subsequent centrifugation at 44 *g* [29]. Hepatocytes were cultured on collagen type I coated dishes with DMEM-F12 supplemented with 10% FCS and 1% antibiotic/antimycotic solution. Sinusoidal endothelial cells (SEC) and liver macrophages (Kupffer cells) were obtained from rat liver after perfusion with collagenase CLS type I (Biochrom) and pronase E (Merck). The cell suspensions were then purified by density gradient centrifugation (20.5% Nycodenz) and centrifugal elutriation essentially as described [30]. The SEC were centrifuged at 1,017 *g*, elutriated at 19–27 mL/min, and finally cultured in endothelial cell growth medium with supplements (PromoCell) on collagen type I-precoated coverslips (Becton Dickinson Labware). Kupffer cells were centrifuged at 1,017 *g*, elutriated at 32–51 mL/min, and subsequently cultured on uncoated glass coverslips using RPMI 1640 medium (Biochrom) supplemented with 10% FCS and 1% antibiotic/antimycotic solution. Umbilical cord blood stem cells were obtained from Wistar rats (20 days *post coitum*) by rinsing the umbilical cord with medium and clonally expanded in DMEM-F12 containing 15% FCS (Stem Cell Technologies), 10 ng/mL rat leukemia inhibitory factor (Millipore), and 1% antibiotic/antimycotic solution. Rat embryonic stem cells (ESC) were purchased from Celprogen and cultured on special dishes in the maintenance medium from Celprogen. The rat hepatoma cell line H4IIE was purchased from the American Tissue and Cell Collection (ATCC) and cultured in DMEM with 10% FCS and 1% antibiotic/antimycotic solution. Muscle fibroblasts were obtained from abdominal muscle of rats by outgrowing and cultured for at least 14 days before use in DMEM containing 10% FCS and 1% antibiotic/antimycotic solution.

Partial hepatectomy

PH was performed by surgical removal of the 2 largest liver lobes (70%–80% of the liver mass) as described [31]. In a second approach, pellets with AAF (70 mg AAF 14 day release; Innovative Research of America, Sarasota, FL) were implanted under the skin of the neck of wild-type Wistar rats (200–250 g body mass) 7 days before PH was performed essentially as described [22,31]. The regeneration of the livers was documented within the first 14 days after PH using 3 different rats for each time point. The livers were perfused with buffer and immediately snap-frozen in liquid nitrogen. Liver tissue was stored at −80°C and subsequently used for the preparation of RNA, protein, and tissue sections. The animal procedures were approved by the local committee for animal protection, and all animals received care according to the German animal welfare act.

Reverse transcriptase–polymerase chain reaction

Total RNA was isolated from time series of cultured HSC and liver tissue samples using the RNeasy Mini Kit (Qiagen). After RNA isolation, the RNA was quantified by spectrophotometry. The first-strand cDNA was made from 1 μg mRNA per 20 μL reaction volume using the RevertAid H Minus First Strand cDNA Synthesis Kit (Fermentas). The polymerase chain reaction (PCR) was performed in 25 μL reaction volume using a standard protocol with 250 ng template cDNA, 0.2 μM of each primer and the 2× PCR Master Mix (Fermentas). The primers used for RT-PCR were designed with the program Primer 3 and indicated in Table 1.

The expression levels of Nestin during liver regeneration were measured by quantitative RT-PCR (qRT-PCR) using the Maxima SYBR Green qPCR Master Mix (Fermentas) and the ABI7500 (Applied Biosystems by Life Technologies) according to the manufacturer's instructions. Hypoxanthine-guanine phosphoribosyltransferase 1 served as a reference. The ΔCt method was used to calculate the expression of Nestin [32]. The primers applied for qRT-PCR were listed in the Table 2.

Western blot

HSC, umbilical cord blood stem cells, and liver tissue were homogenized in lysis buffer [10 mM 4-(2-hydroxyethyl)-1-piperazineethanesulfonic acid, 10 mM KCl, 1.5 mM $MgCl_2$, 0.5 mM dithiotreitol, 0.01% nonylphenoxypolyethylenglycol, and 1 μg/mL phenylmethanesulfonylfluoride] and incubated on ice for 10 min to enrich cytosolic/cytoskeletal proteins essentially as described [33]. This protein fraction was

Table 1. Primers for Reverse Transcriptase–Polymerase Chain Reaction

Gene	Forward primer	Reverse primer	bp	Accession no.
α-SMA	TGCTGGACTCTGGAGATG	GTGATCACCTGCCCATC	292	X06801
β-actin	GCCCTAGACTTCGAGCAAGA	CAGTGAGGCCAGGATAGAGC	390	NM_031144
CD133	TTAATGCAGCACCAGGTACATC	TCGTTGAGCAGGTAGGGAGTAT	370	NM_021751
Col1α2	ACCTCAGGGTGTTCAAGGTG	CGGATTCCAATAGGACCAGA	222	NM_053356
FBX15	GTCCACCCTGAATTTGTATGGT	AGTCCATACTCTGGGCTGTCAT	467	NM_001108436
GDF3	ACCTGCAGGGTGTGGTTAAG	TGCATGAAGGCATAATTGGA	400	NM_001109671
GFAP	ACATCGAGATCGCCACCTAC	TCCACCGTCTTTACCACGAT	163	L27219
KLF4	CCAGGACTACCCCTACACTGAG	CACAGCCTGCATAGTCACAAGT	273	NM_053713
MYC	GAGCTACTTGGAGGAGACATGG	TCTTTTCCACAGACACCACATC	496	NM_012603
Nestin	GAGTGTCGCTTAGAGGTGCAA	TGTCACAGGAGTCTCAAGGGTA	450	NM_012987
Notch1	AGAGCTTTTCCTGTGTCTGTCC	CGGTACAGTCAGGTGTGTTGTT	414	NM_001105721
Notch3	CCTCTTTCACCTGTACCTGTCC	ACACAGTAGTGGGAGTGGTCCT	496	NM_020087
OCT4	GCTGAAACAGAAGAGGATCACC	TACAGAACCACACTCGAACCAC	354	NM_001009178
SOX2	AACGGCAGCTACAGCATGA	TGGTTACCTCTTCCTCCCACT	280	NM_001109181

centrifuged and the supernatant was used for Western blot analysis after protein quantification according to Bradford [34]. This fraction contained the highest Nestin concentration. The cell lysates were then separated and transferred to nitrocellulose using a tank blot apparatus. Antibodies against Nestin (Santa Cruz Biotechnologies) glyceraldehyd-3-phosphate dehydrogenase (Millipore), and γ-tubulin (Sigma-Aldrich) were used for the immunoblots. A secondary goat anti-mouse antibody conjugated with horseradish peroxidase (Bio-Rad Laboratories) was administered and enhanced chemoluminescence detection reagents with chemoluminescence sensitive films (GE Healthcare Europe) were used to visualize marked protein bands. The band intensity of 3 different experiments was quantified using the LabImage software (Kappelan Bio Imaging).

Immunofluorescence

HSC, H4IIE, umbilical cord blood stem cells, hepatocytes, SEC, Kupffer cells, and muscle fibroblasts were cultured on coverslips for 1, 2, or 7 days. After washing with phosphate-buffered saline (PBS) the cells were fixed with ice-cold methanol and incubated with 10% rat serum in PBS. Cryosections (10 μm thickness) of the perfused rat liver were treated in a similar manner. Afterward, the samples were incubated with antibodies against Nestin, α-SMA (Sigma-Aldrich), CD133 (Abcam), cytokeratins (panCK; Dako), desmin (Dako), GFAP (Millipore), major histocompatibility complex class II (MHC II; Abcam), rat endothelial cell antigen 1 (Santa Cruz Biotechnologies), or sodium-taurocholate cotransporting polypeptide (Santa Cruz Biotechnologies) dissolved in 2% rat serum. Subsequently, the cells and tissue sections were incubated with donkey anti-mouse and/or anti-rabbit (Millipore) antibodies, conjugated with the fluorescent dye cyanine 3 or fluorescein isothiocyanate, and diluted in 2% rat serum. The cells and tissue samples were covered with ProLong Gold Mounting Medium containing 4′, 6-diamidino-2-phenylindole (Molecular Probes, Invitrogen).

DNA methylation

The cultured cells were rinsed with PBS and then harvested using a cell scraper. Genomic DNA was isolated using the DNeasy Blood and Tissue Mini Kit (Qiagen). The DNA was quantified and 2 μg of DNA were used for bisulfite (BS) conversion using the EpiTect Bisulfite Kit (Qiagen) according to the manufacturer's instructions. The converted DNA was collected in 30 μL buffer and stored at −20°C. For BS sequencing the primers shown in Table 3 were used with the Phire Hot Start PCR Mastermix (Finnzymes) using 5 μL of BS DNA in a standard PCR protocol. The primers for BS sequencing were designed using the program Meth-Primer [35]. The PCR products were separated by gel electrophoresis, and the product band was excised and subsequently purified using the Wizard SV Gel Elution Kit (Promega). The purified PCR product was finally sequenced.

Histone H3 methylation

Chromatin immunoprecipitations (ChIP) were used to investigate epigenetic regulation by histone H3 methylation at lysine 4 (K4) and 9 (K9). The chromatin was cross-linked by 1% formalin and applied for ChIP analysis using the ChIP-IT Kit (Active Motif) according to the manufacturer's guidelines. After an enzymatic shearing the chromatin was mixed with antibodies against either H3K4me3 or H3K9me3 (Abcam). Antibodies against the RNA polymerase II and unspecific mouse immunoglobulins (Active Motif) were used as precipitation controls. The antibody–antigen complexes were precipitated by magnetic beads. The DNA was extracted and

Table 2. Primers for Quantitative Reverse Transcriptase–Polymerase Chain Reaction

Gene	Forward primer	Reverse primer	bp	Accession no.
HPRT1	TGCTCGAGATGTCATGAAGGA	CAGAGGGCCACAATGTGATG	51	NM_012583
Nestin	AGGAAGAAGCTGCAGCAGAG	TCTGGCATTGACTGAGCAAC	160	NM_012987

Table 3. Primers for Bisulfite Sequencing

Gene	Forward primer	Reverse primer	bp	Accession No.
CD133	TTTTGGGGTTGGATTTTAAATAAT	AAACCAAAACTTCTAACCCCTATAC	717	NM_021751
Nestin	GGGGTGTTTGGTTGTATTTTAAG	AAACTCCCACATCTAAAAAAATTCTT	388	NM_012987
Notch1	TTGATTTTTAGTATGGGGTTTTAGG	CAAATATACAACCCCATTCACAATA	812	NM_001105721
Notch3	AGGTGATTGATGTTTAGTGTTTTTA	ACAACCCCAAACTACTACCTACTAC	764	NM_020087

used for a quantitative PCR with primers for Nestin and glyceraldehyd-3-phosphate dehydrogenase (Table 4) using the Maxima qPCR Master Mix. The results were interpreted by normalizing the expression of the Nestin PCR products of precipitated samples against the Nestin PCR products of input DNA without antibody precipitation.

Statistics

Parametric analysis (Student's *t*-test) was used for paired statistical analysis of the data ($P < 0.05$). The means of at least 3 independent experiments and the standard error of mean were indicated.

Results

Stem cell factors in quiescent and activated HSC

HSC cultured for 1 day express the stellate cell marker *GFAP* along with *CD133* and *Notch1* (Fig. 1A). CD133 is a marker of stem/progenitor cells and was also detected in clonally expanded umbilical cord blood stem cells of rats (clone 1G11) as demonstrated by RT-PCR and immunofluorescence staining (Fig. 1B, H). The clone 1G11 expressed also factors associated with pluripotency such as octamer binding factor 4, sex determining region Y-box 2, *MYC*, and Krüppel-like factor 4. The expression of *FBX15* (F-box only protein 15), which is known to be controlled by simultaneous activity of octamer binding factor 4 and sex determining region Y-box 2, further confirms the expression of these transcription factors in 1G11 cells. The transcription of growth and differentiation factor 3 in these umbilical cord blood stem cells was also indicative for their high developmental potential (Fig. 1B).

Activated HSC were generally characterized by the expression of myofibroblast markers in many studies. Indeed, α-SMA and the connective tissue protein collagen type 1 α2 chain (Col1α2) were induced in HSC during their activation in culture. The culture-dependent activation process was further confirmed by Western blot analysis of Nestin, which is known to be represented by different protein bands. Nestin protein levels were very low in freshly isolated HSC and increased during time in culture (Fig. 1C). The protein Nestin was also detectable in the umbilical cord blood stem cells (clone 1G11; Fig. 1C). In addition to the Western blots, RT-PCR analysis of HSC cultured for 1 day as well as ESC and umbilical cord blood stem cells of rats were performed. Nestin mRNA was detectable in most HSC preparations after 1 day of culture and in clones of umbilical cord blood stem cells, but not in ESC (Fig. 1D). The induction of Nestin during culture-dependent activation of HSC was further confirmed by immunofluorescence staining. Freshly isolated HSC displayed no Nestin staining (Fig. 1E), whereas all HSC contained Nestin filaments after 7 days of culture. Nestin levels were lower in HSC that displayed 2 nuclei per cell (Fig. 1F). The expression of Nestin by all activated HSC (Fig. 1F) and all umbilical cord blood stem cells (Fig. 1G) indicated homogeneous cell populations in both cases. The purity of isolated HSC was further confirmed by their vitamin A content. HSC cultured for 2 days contained lipid droplets that displayed vitamin A autofluorescence in all cells (Fig. 2A). Moreover, the uniform expression of GFAP at the second day of culture indicates the purity of HSC also. At this time point, the isolated HSC had already begun to synthesize Nestin (Fig. 2B). Other cell types of the liver such as parenchymal cells, SEC, and Kupffer cells could be identified by their typical cell markers like sodium-taurocholate cotransporting polypeptide, rat endothelial cell antigen 1, or MHC II, respectively, but were negative for Nestin as demonstrated by immunofluorescence stainings (Fig. 2C–E). Also, α-SMA-expressing muscle fibroblasts displayed no Nestin synthesis (Fig. 2F), indicating that the occurrence of Nestin in HSC and umbilical cord blood stem cells was not associated with culture artifacts.

Nestin expression during liver regeneration

Since Nestin is only expressed by activated stellate cells of the rat liver, we used this marker to study their activation during liver regeneration after PH. The immunofluorescence staining of liver sections showed that Nestin was only barely detectable at the first day of regeneration (Fig. 3A), but Nestin synthesis increased strongly 1 day later (Fig. 3B). The staining pattern showed a clear sinusoidal staining of cells with distinct cellular processes, which gave another hind toward

Table 4. Primers for Chromatin Immunoprecipitation Analysis

Gene	Forward primer	Reverse primer	bp	Accession no.
GAPDH1	ACTGGCCACGCTAATCTGAC	TGACCTTGAGGTCTCCTTGG	292	NM_017008.2
GAPDH2	AGACAGCCGCATCTTCTTGT	CCCCCATTCCTAATTTCCAT	390	NM_017008.2
Nestin1	GGGCCACTCCCTTCTCTAGT	AGCAGCTGGTTTTGCTCTTC	370	NM_012987
Nestin2	GGCTGCACTTTGGTTCTTCT	CCCAGGCCTTAACCCTTTAG	222	NM_012987

stellate cells. After the maximum of Nestin expression was reached at the third day of regeneration (Fig. 3C), the Nestin expression decreased from the fourth to the sixth day (Fig. 3D–F) and remained low during the second week of regeneration (Fig. 3G–I). In contrast to this, the Nestin expression was more pronounced after application of AAF followed by PH. Elevated Nestin levels were detected in the liver from day 2 to 14 of liver regeneration in this model (Fig. 4A–I). The maximum of Nestin expression was found around day 7 in the vicinity of portal tracts (Fig. 4G). The contribution of stellate cells to the increased expression of Nestin during tissue regeneration in both models of liver injury was verified by co-staining of Nestin and the stellate cell marker desmin using confocal laser scanning microscopy (Fig. 5A–C). Nestin-positive HSC surrounded cells that expressed cytokeratins (panCK) and spread in ducts 7 days after PH in the presence of AAF. The immunofluorescence stainings of Nestin and panCK were found to be distinct (Fig. 5D).

To verify the increased expression of Nestin during liver regeneration as suggested by immunofluorescence stainings, Western blot analysis were performed. The immunoblots showed a comparable progression of Nestin synthesis as determined by immunofluorescence staining with a maximum at the third day of regeneration after PH. Nestin expression was low in the normal (0 day) and regenerated liver (10–14 day) (Fig. 6A). In the second model of liver regeneration, the AAF treatment followed by PH induced high levels of Nestin expression from day 2 to 14 (Fig. 6B). To quantify the protein amount of Nestin during liver regeneration a densitometric analysis of a prominent Nestin protein

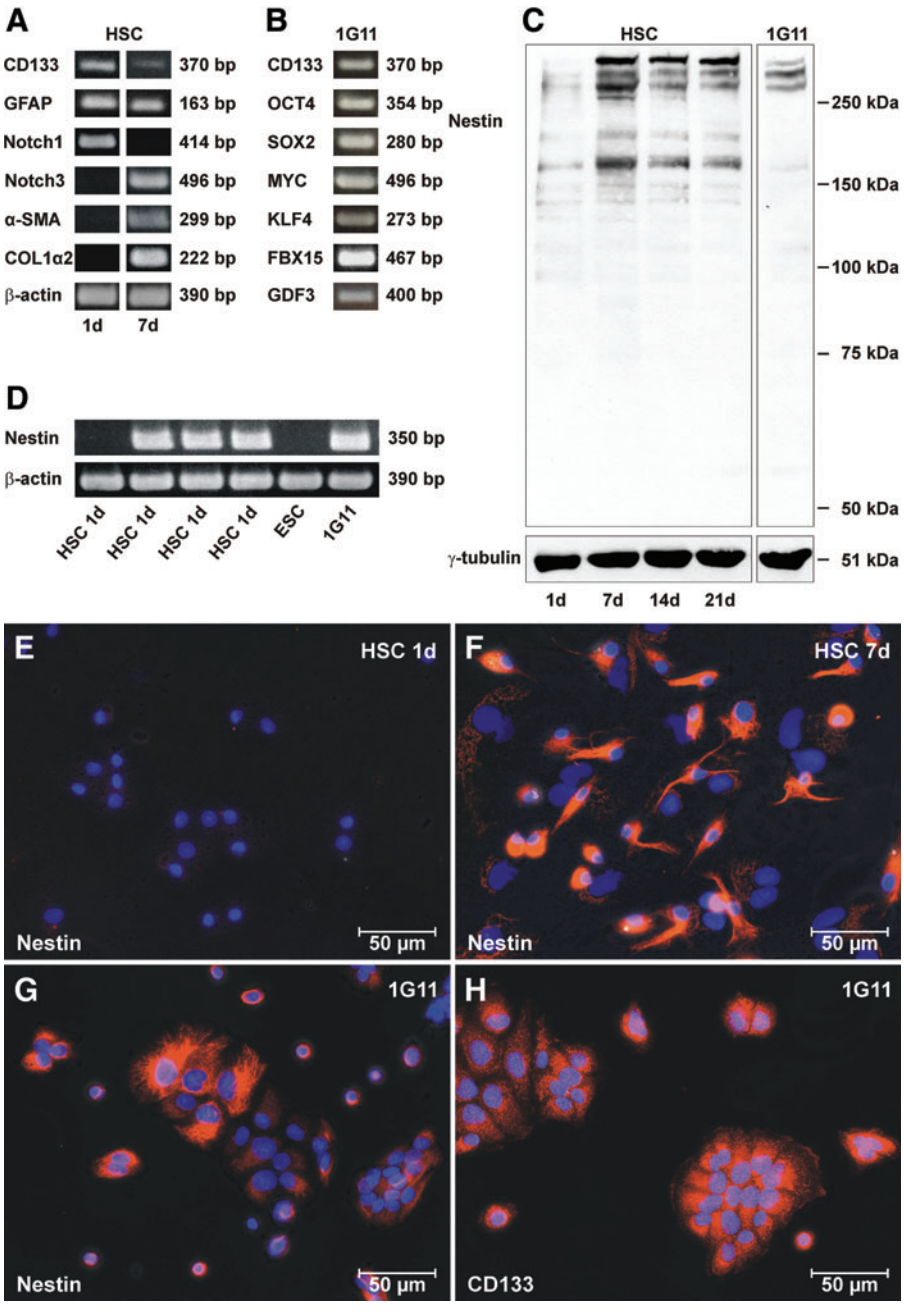

FIG. 1. Characterization of quiescent and activated HSC as well as umbilical cord blood stem cells (1G11). **(A)** Expression analysis of CD133, GFAP, Notch1, Notch3, α-SMA, and Col1α2 in quiescent (1 day) and culture-activated (7 day) HSC by RT-PCR. The RT-PCR of β-actin served as a control. **(B)** Umbilical cord blood stem cells of the clone 1G11 expressed CD133 and factors known from pluripotent cells such as OCT4, SOX2, MYC, KLF4, FBX15, and GDF3 as investigated by RT-PCR analysis. **(C)** Analysis of Nestin by Western blot in HSC after 1, 7, 14, and 21 days of culture as well as in 1G11 cells. The protein γ-tubulin served as a control. **(D)** RT-PCR analysis of Nestin in 4 different HSC preparations after 1 day of culture as well as ESC and 1G11 cells. The mRNA of β-actin served as a control. Immunofluorescence staining of Nestin in HSC cultured for **(E)** 1 and **(F)** 7 days as well as **(G)** 1G11 cells (red). **(H)** 1G11 cells expressed also CD133 as determined by immunofluorescence staining (red). The cell nuclei were counterstained by DAPI (blue). HSC, hepatic stellate cells; ESC, embryonic stem cells; GFAP, glial fibrillary acidic protein; α-SMA, α-smooth muscle actin; RT-PCR, reverse transcriptase-polymerase chain reaction; DAPI, 4′, 6-diamidino-2-phenylindole; GDF3, growth and differentiation factor 3; KLF4, Krüppel-like factor 4; SOX2, sex determining region Y-box 2; OCT4, octamer binding factor 4. Color images available online at www.liebertonline.com/scd

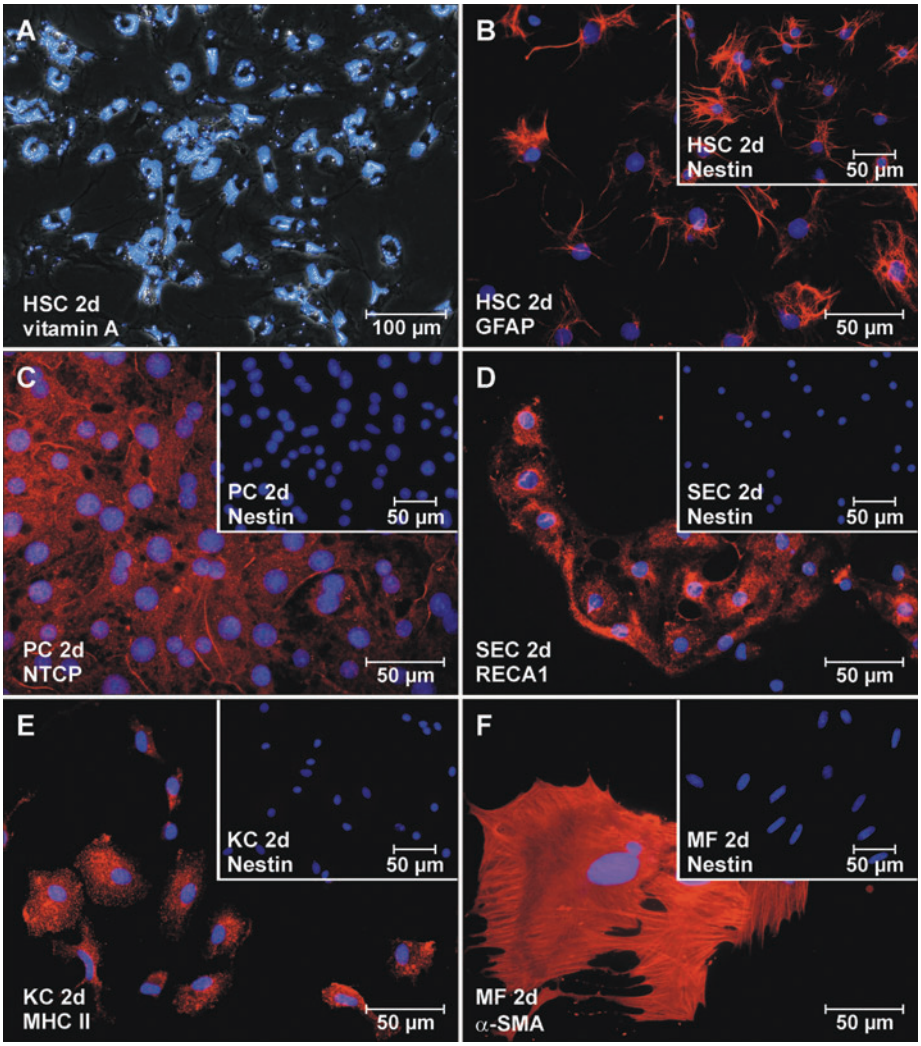

FIG. 2. Nestin immunofluorescence staining of different liver cell types and muscle fibroblasts obtained from rats. **(A)** The vitamin A droplets of isolated HSC after 2 days (2 day) of culture was observed after excitation with UV light at 350 nm through rapidly fading fluorescence light (light blue). The vitamin A fluorescence was combined with phase-contrast transmission light microscopy. **(B)** HSC cultured for 2 days expressed GFAP as demonstrated by immunofluorescence staining and started to synthesize Nestin (upper right hand corner) also (red). In contrast to this, no isolated **(C)** parenchymal cells (PC; NTCP), **(D)** SEC (RECA1), **(E)** Kupffer cells (KC; MHC II), or **(F)** muscle fibroblasts (MF; α-SMA) were stained with antibodies against Nestin (upper right hand corner) after 2 days of culture. The cell nuclei were stained by DAPI (blue). RECA1, rat endothelial cell antigen 1; NTCP, sodium-taurocholate cotransporting polypeptide. Color images available online at www.liebertonline.com/scd

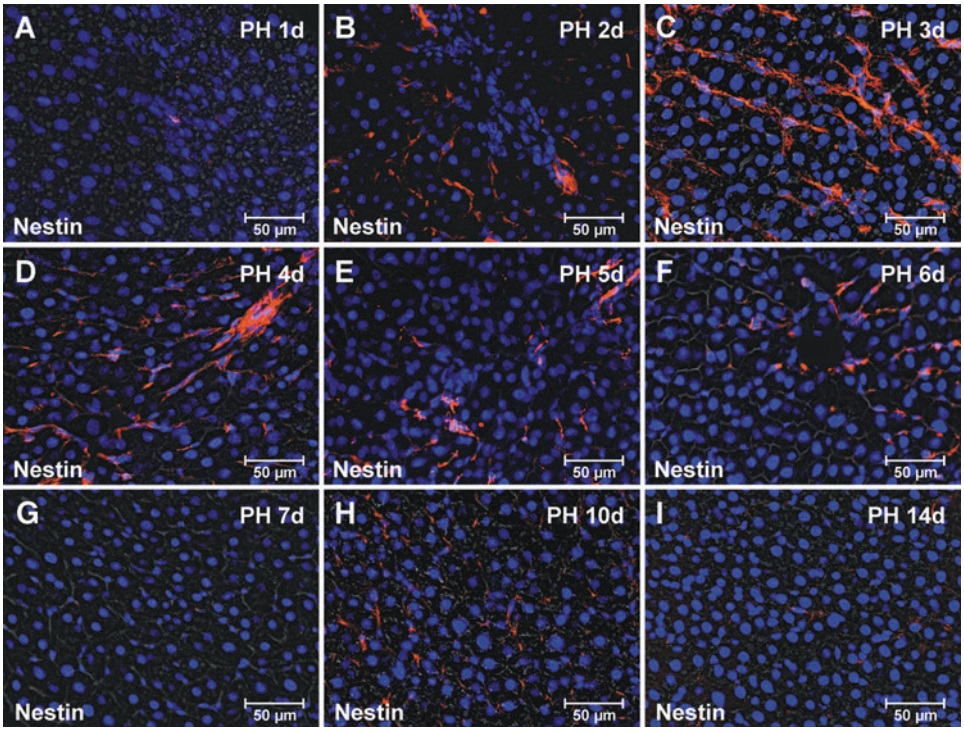

FIG. 3. Immunofluorescence staining of Nestin during liver regeneration after partial hepatectomy (PH). **(A–I)** Cryosections of regenerating rat livers were stained with antibodies against Nestin (red) at the time points indicated. The cell nuclei were stained by DAPI (blue). Color images available online at www.liebertonline.com/scd

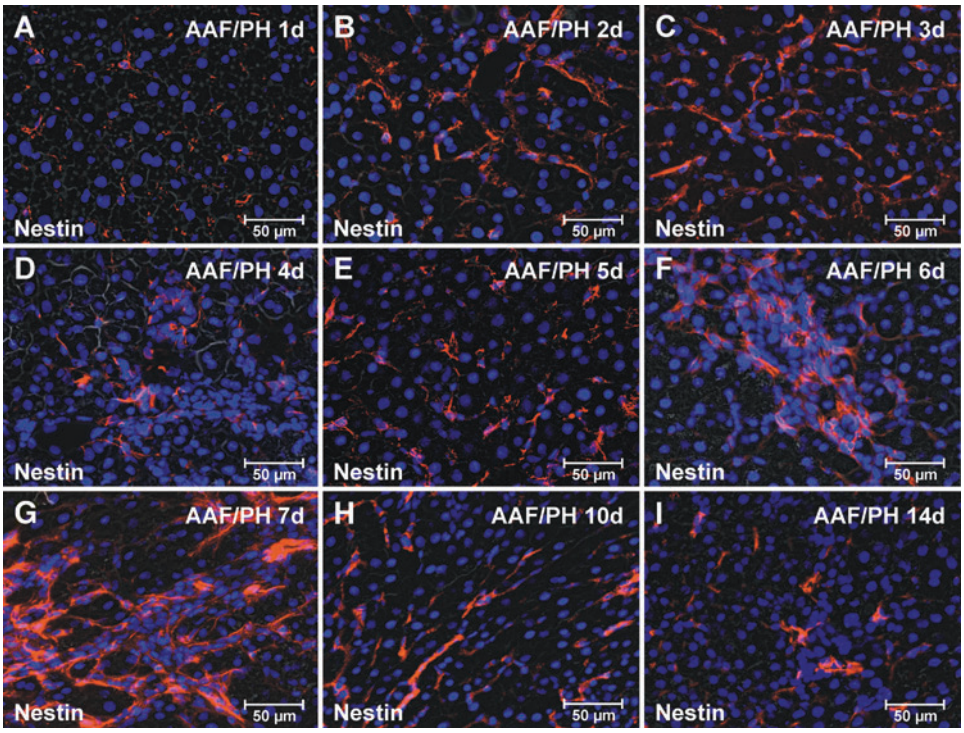

FIG. 4. Immunofluorescence staining of Nestin during liver regeneration after PH in the presence of AAF. **(A–I)** Cryosections of regenerating rat livers were stained with antibodies against Nestin (red) at the time points indicated. The cell nuclei were stained by DAPI (blue). AAF, 2-acetylaminofluorene. Color images available online at www.liebertonline.com/scd

band of about 220 kDa (indicated by an arrow head) was performed. Nestin levels from total liver were significantly elevated from the second to the fifth day of regeneration after PH compared to the normal liver (Fig. 6C). The densitometric analysis of Nestin Western blots after PH in the presence of AAF documented significantly higher amounts of Nestin protein from the 2nd to the 14th day of regeneration compared to the application of AAF without PH (0 day) (Fig. 6D). The Nestin induction in both models of liver regeneration was also confirmed by qRT-PCR analysis, which revealed the highest Nestin mRNA levels from the first to third day of regeneration after PH (Fig. 6E) and from the sixth to seventh day of regeneration after PH under AAF (Fig. 6F).

Regulation of Nestin by epigenetic mechanisms

The BS sequencing analysis of *Nestin* DNA from freshly isolated and cultured HSC displayed no DNA methylation at any time point investigated (Fig. 7A), although Nestin was not detectable by immunofluorescence staining or Western blot in freshly isolated HSC, indicating that other mechanisms are involved in the regulation of Nestin synthesis. Clones of umbilical cord blood stem cells (1G11) synthesize Nestin (Fig. 1C, G) and displayed no detectable DNA methylation (Fig. 7A). Also, the ESC showed no or low DNA methylation, but Nestin was not expressed in this cell type (Fig. 1D). In contrast to this, differentiated cells such as hepatocytes displayed a methylation of the *Nestin* DNA and, in accordance with this, no Nestin expression (Fig. 7A). The strongest DNA methylation was detected in the hepatoma cells H4IIE, where most cytosines of CpG are methylated (Fig. 7A). In agreement with this, neither the mRNA nor the protein of Nestin was detectable (Fig. 7B, C). To investigate if DNA methylation can control transcription of the *Nestin* gene, H4IIE cells were cultured with the DNA methylation

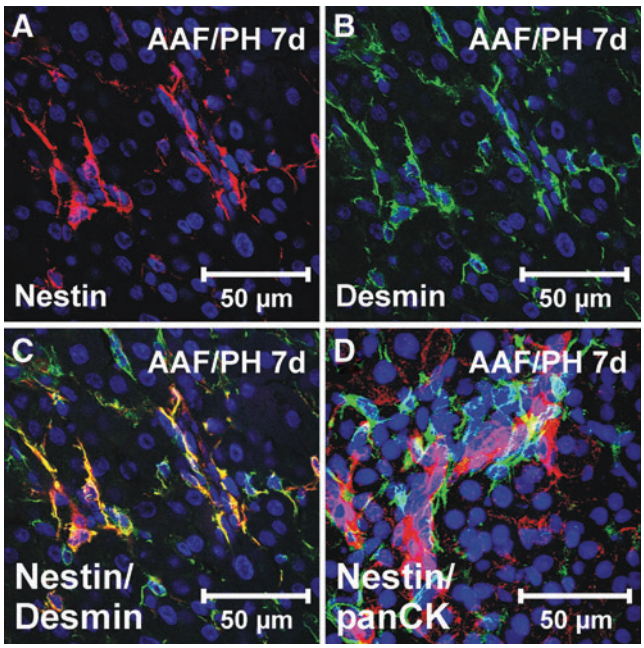

FIG. 5. Identification of Nestin-expressing HSC during liver regeneration. **(A)** Nestin (red) and **(B)** desmin (green) costaining of liver sections with fluorescence-labeled antibodies 7 days (7 day) after PH in the presence of AAF. The fluorescence images were taken by confocal laser scanning microscopy and **(C)** finally merged. **(D)** Cytokeratin-expressing cells (panCK; red) that appeared in the AAF/PH model after 7 days in the vicinity of portal tracts displayed no Nestin (green) expression as determined by 3-dimensional rendering of images series made by confocal laser scanning microscopy. The cell nuclei were counterstained by DAPI (blue). Color images available online at www.liebertonline.com/scd

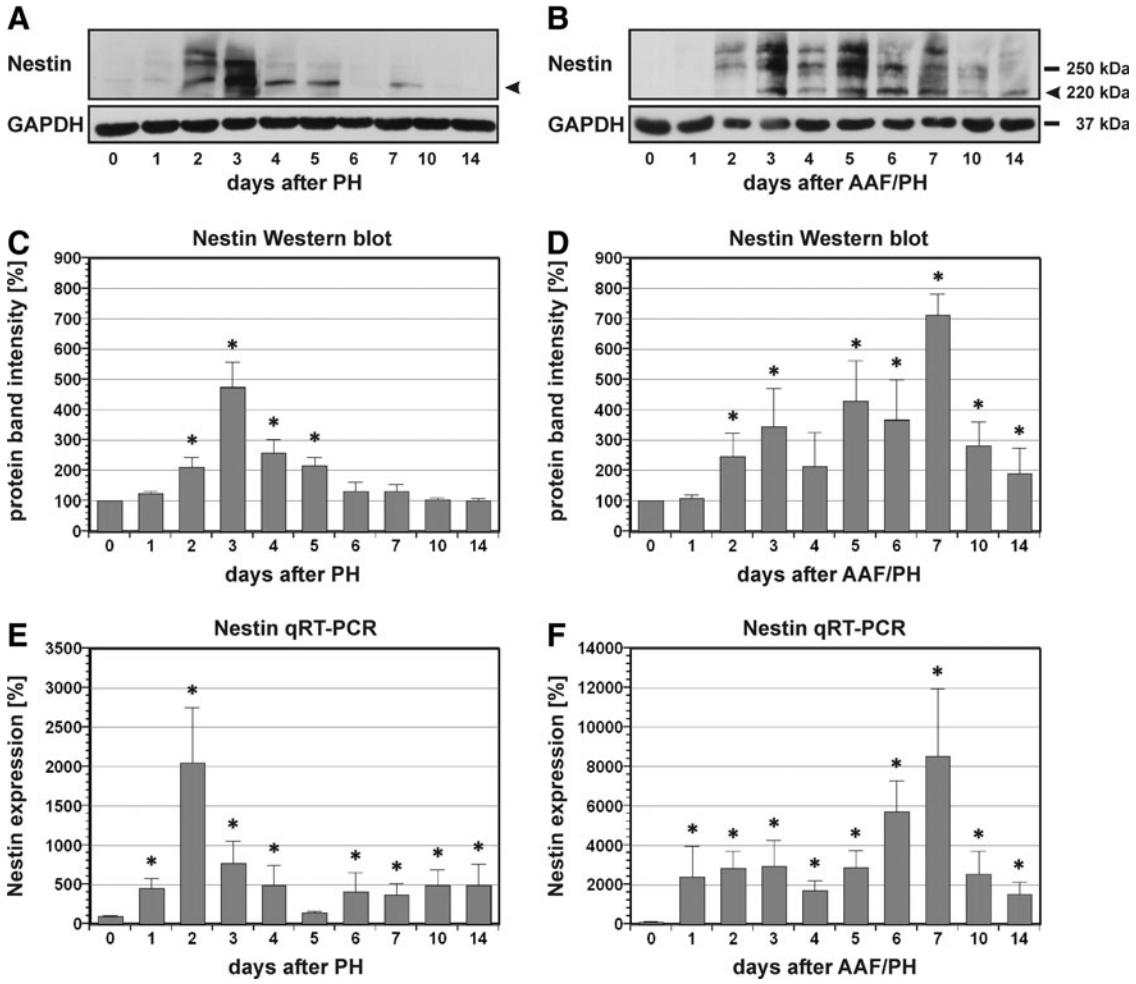

FIG. 6. Detection of Nestin by Western blot and quantitative RT-PCR after PH in the absence **(A, C, E)** and presence of AAF **(B, D, F)**. Nestin was analyzed by Western blot in whole liver (200 µg protein of cytosolic/cytoskeletal fractions) after **(A)** PH and **(B)** PH with application of AAF. The protein GAPDH served as a control. Western blot analysis of Nestin synthesis during liver regeneration after **(C)** PH and **(D)** PH with AAF treatment. The protein band (~220 kDa) indicated by an arrow head was used for densitometric analysis ($n = 3$; $^*P < 0.05$ in comparison to the liver before PH, 0 day). Analysis of the Nestin expression by quantitative RT-PCR in samples of whole liver after **(E)** PH and **(F)** PH in the presence of AAF ($n = 3$; $^*P < 0.05$ in comparison to the liver before PH, 0 day). The expression analyses were normalized with the housekeeping gene *HPRT1* ($n = 3$; not shown). GAPDH, glyceraldehyd-3-phosphate dehydrogenase; HPRT1, hypoxanthine-guanine phosphoribosyltransferase 1.

inhibitor 5-Aza-2-deoxycytidine (Aza). After 72 h of culture in presence of 5–10 µM Aza, Nestin was induced in H4IIE cells as determined by RT-PCR and immunofluorescence staining (Fig. 7B, D). All H4IIE cells treated with 10 µM Aza were Nestin-positive after 72 h (Fig. 7D). This confirmed in principle the possibility of an epigenetic regulation of *Nestin* by DNA methylation. In undifferentiated cells, however, the DNA methylation is apparently replaced by other regulatory mechanisms. To investigate a possible epigenetic regulation of *Nestin* by histone H3 methylation, antibodies against 3 methyl groups of lysine 4 (K4) or lysine 9 (K9) of histone H3 were used for immunoprecipitation of chromatin. The genomic *Nestin* nucleotide sequence of precipitated DNA was then analyzed by quantitative PCR. The use of H3K4me3 antibodies, which detected activating histone H3 methylation, enriched about 3-fold higher levels of *Nestin* DNA from HSC cultured for 7 days compared to HSC cultured for 1 day (Fig. 8A). In contrast to this, H3K9me3 antibodies directed against inhibitory histone H3 methylation showed a decrease of the precipitated *Nestin* DNA by 79% ± 12% in culture-activated HSC (7 day) compared to quiescent HSC (1 day; Fig. 8B). Compared with lysine 4, the lysine 9 of histone H3 is highly methylated in ESC (Fig. 8C). The results of this ChIP analysis suggested regulation of *Nestin* expression by histone H3 methylation in HSC and ESC.

Regulation of CD133 and Notch receptors by DNA methylation

The regulation of *CD133* expression by DNA methylation was also investigated in HSC. The DNA sequence of *CD133* was not methylated in freshly isolated HSC (1 day, Fig. 9A). After 1 week of culture, the DNA methylation of *CD133* was 25% ± 2% and increased up to 37% ± 9% on the 14th day of

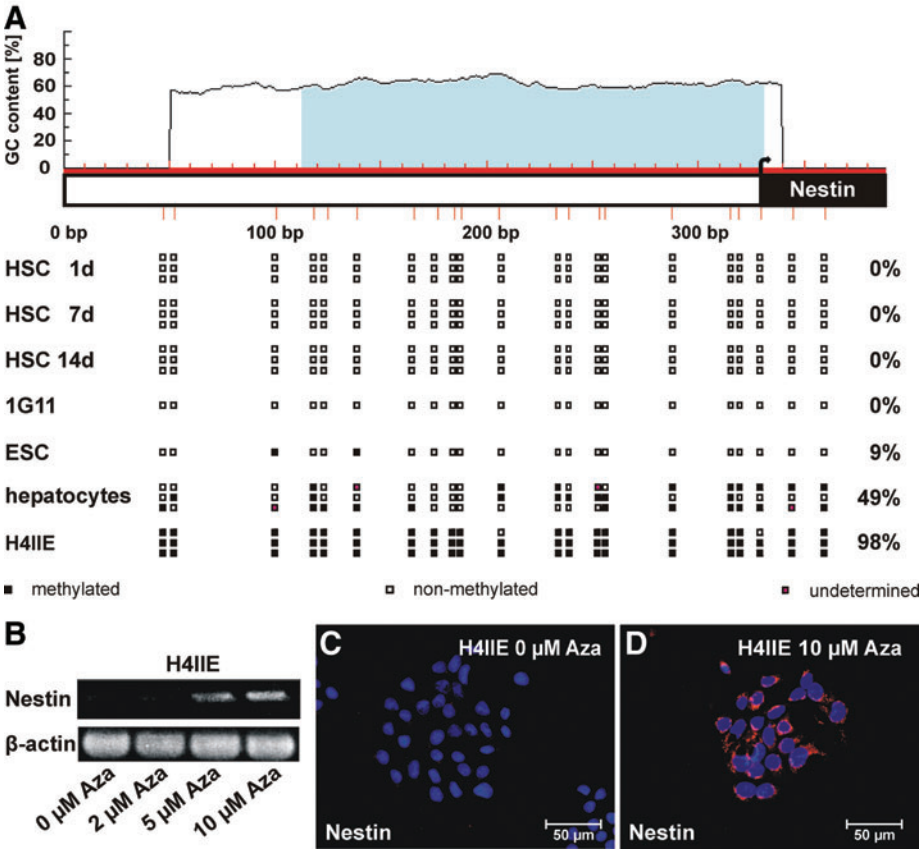

FIG. 7. Regulation of the *Nestin* expression by DNA methylation. **(A)** Analysis of *Nestin* DNA methylation by bisulfite sequencing in HSC on the 1st, 7th, and 14th day of culture as well as the umbillical cord blood stem cell clone 1G11, ESC, hepatocytes, and H4IIE hepatoma cells. Hepatocytes were cultured for 1 day before analysis ($n = 3$). A CpG rich region was highlighted in blue. The positions of CpG were marked with red bars. Methylated CpG are labeled with black squares, whereas open squares represent unmethylated CpG. Red squares indicated undetermined methylation of CpG. The coding region of the gene was highlighted in black, and the transcription initiation site was indicated by an arrow. **(B)** Induction of Nestin expression in H4IIE cells by Aza treatment for 72 h as investigated by RT-PCR. β-actin served as a control. Immunofluorescence staining of Nestin (red) in H4IIE cells **(C)** without and **(D)** with 10 µM Aza for 72 h. The cell nuclei were stained by DAPI (blue). CpG, cytosine phosphatidyl guanosine; Aza, 5-Aza-2-deoxycytidine. Color images available online at www.liebertonline.com/scd

culture. This result was in good agreement with the transcriptional silencing of *CD133* in culture-activated HSC (Fig. 1A). *Notch1*, a marker for quiescent stem cells and freshly isolated HSC (Fig. 1A), was barely methylated in HSC cultured for only 1 day (2% ± 1%; Fig. 9B). The *Notch1* expression became apparently repressed by DNA methylation during culture of HSC. The methylation level of *Notch1* DNA was 57% ± 10% in HSC cultured for 7 days (Fig. 9B), indicating a regulation of *Notch1* expression by DNA methylation in HSC. In contrast to *Notch1*, the DNA methylation level of *Notch3* was about 51% ± 5% in quiescent HSC. The DNA at the *Notch3* locus became demethylated in HSC cultured for 7 days. Culture-activated HSC displayed only 5% ± 1% of *Notch3* DNA methylation (Fig. 9C). This enabled the expression of *Notch3* in HSC cultured for 7 days as demonstrated by RT-PCR (Fig. 1A). The expression of *Notch1* and *Notch3* receptors in HSC is apparently controlled by DNA methylation, but the genes were found to be differentially regulated in quiescent and activated HSC, resulting in a shift from Notch1 to Notch3 during HSC activation.

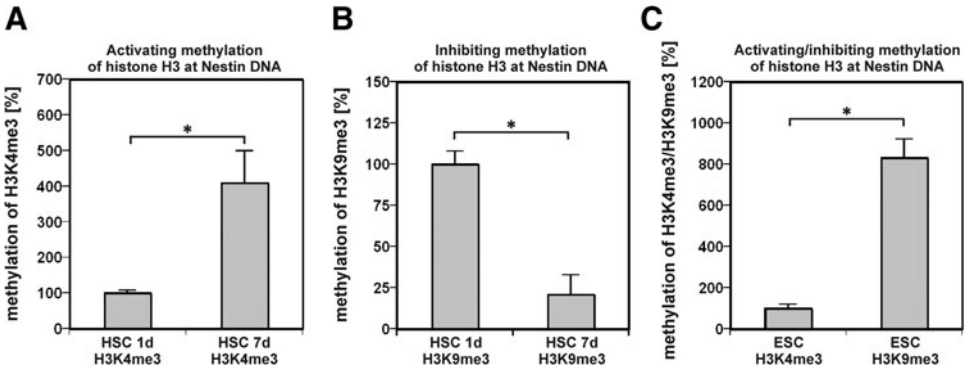

FIG. 8. Chromatin immunoprecipitation analysis of the histone H3 lysine methylation in HSC and ESC at the *Nestin* locus of the DNA. Chromatin was harvested from quiescent (1 day) and culture-activated (7 day) HSC as well as cultured ESC from rats. **(A)** The chromatin was immunoprecipitated with antibodies against H3K4me3, an activating methylation of lysine 4 (K4) of histone H3, and **(B)** H3K9me3, an inhibitory methylation of the lysine 9 (K9) of histone H3. The diagrams show the relative enrichment of *Nestin* DNA with antibodies normalized against the input *Nestin* DNA without immunoprecipitation as determined by quantitative PCR ($n = 3$; $P < 0.05$). **(C)** Analysis of the activating (H3K4me3) and inhibiting methylation (H3K9me3) of histone H3 at the *Nestin* locus of the DNA obtained from rat ESC ($n = 3$; $^*P < 0.05$).

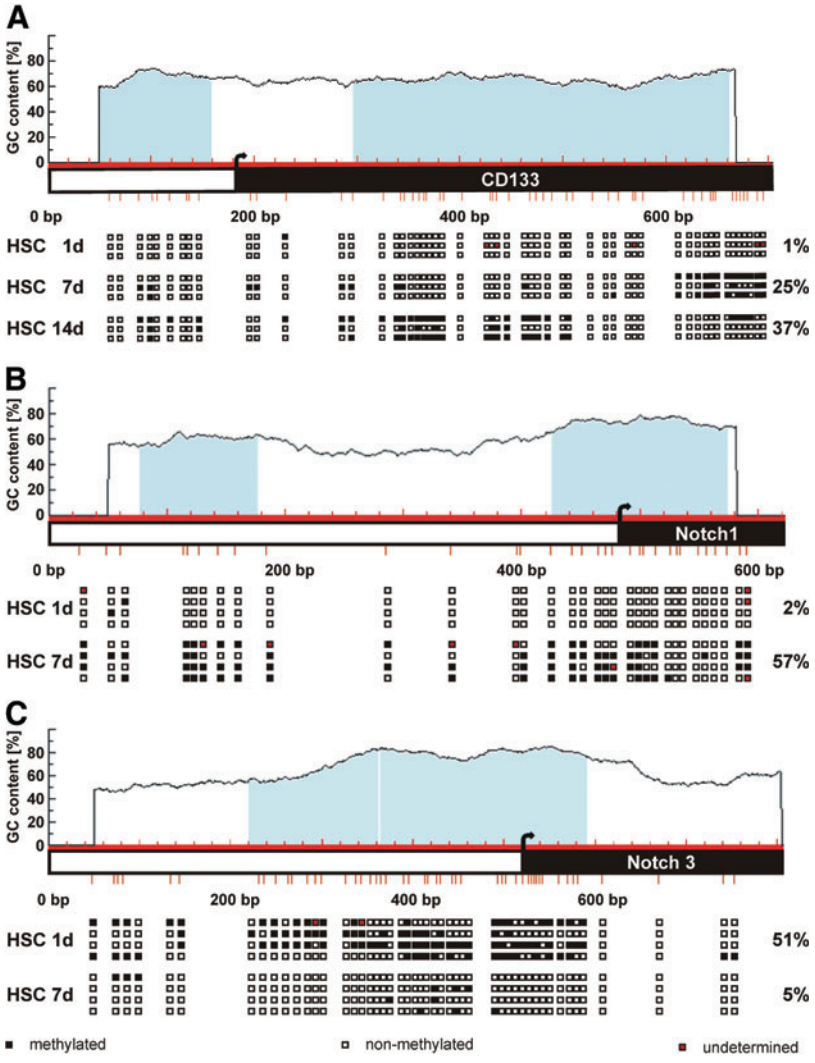

FIG. 9. DNA methylation analysis of *CD133*, *Notch1*, and *Notch3* in HSC. The DNA methylation was analyzed by bisulfite sequencing. **(A)** Methylation analysis of *CD133* DNA in HSC cultured for 1, 7, and 14 days ($n = 3$). Analysis of **(B)** *Notch1* DNA and **(C)** *Notch3* DNA methylation in HSC cultured for 1 and 7 days ($n = 4$). CpG rich regions were highlighted in blue. The positions of CpG were marked with red bars. Methylated CpG are labeled with black squares, whereas open squares represent unmethylated CpG. Red squares indicated undetermined methylation of CpG. The coding regions of the genes were highlighted in black and the transcription initiation site was indicated by an arrow. Color images available online at www.liebertonline.com/scd

Discussion

Origin and identity of liver stem/progenitor cells is under discussion since many years. It was recently demonstrated that HSC express molecular markers of stem/progenitor cells and possess a differentiation potential as documented in vitro and in vivo [16,36]. Little information is available about the regulation of the expression of stem/progenitor cell-associated markers in HSC thus far. It is known that the expression of *CD133* and *Notch1* is downregulated during culture-dependent activation of HSC on plastic [19]. Activated stellate cells start to synthesize α-SMA as well as collagen type I and are, therefore, thought to contribute to liver fibrosis. However, this activation process is impeded in HSC cocultured with hepatocytes or after stimulation of the β-catenin-dependent Wnt signaling pathway. Under these conditions the expression of the stem/progenitor cell markers CD133 and Notch1 is sustained [19,37]. As demonstrated in the present study, epigenetic mechanisms such as DNA methylation are apparently involved in the regulation of *CD133* and *Notch1* during HSC activation. This is most likely an essential molecular mechanism that leads to decreased expression of both stem/progenitor cell factors during culture of HSC on plastic.

It is well known from tumor cells that the expression of *CD133* is regulated by DNA methylation. To get a clear picture of the DNA methylation status of a given gene, cell clones or cell lines are often preferred. In contrast to this, heterogeneous cell populations provide variable results. This is exemplified, for instance, by *Nestin* DNA methylation analysis in isolated hepatocytes that can be less efficiently purified compared to other liver cell types such as HSC, SEC, and Kupffer cells. In primary cultures of hepatocytes the *Nestin* DNA methylation pattern varied between different cell preparations as observed in the present study. In contrast to this, a homogeneous DNA methylation pattern was found in freshly isolated HSC as observed for *CD133*, *Nestin*, and both *Notch* receptors. This was a good indicator for a pure cell population and further proved the expression of *CD133* in stellate cells of the liver. Interestingly, the DNA methylation pattern of *CD133* DNA varied at different time points of activation (ie, between HSC cultured for 7 and 14 days). The reason for this differential *CD133* DNA methylation pattern is unknown yet, but might be associated with a beginning

loss of the developmental potential of many isolated HSC through culture on plastic. This was also indicated by decreased Nestin synthesis in cells with 2 or more nuclei. In contrast to this, CD133 is capable to repress cell differentiation as demonstrated for neuroblastoma cells very recently [38] and at least in part explain the prevalence of CD133 in freshly isolated HSC. Notch1 represents another marker for the quiescent and undifferentiated state of stem/progenitor cells [39]. Therefore, the absence of *Notch1* DNA methylation in quiescent HSC is in good agreement with the undifferentiated state of these cells. Compared with this, Notch3 is involved in the differentiation of hematopoetic stem cells [27] and became upregulated after DNA demethylation during activation of HSC in culture as demonstrated in the present study. This may represent a first step of HSC differentiation or an altered developmental potential during culture on plastic.

Nestin is widely accepted as a marker of activated HSC [20], but not of quiescent HSC that express GFAP in rats. The *Nestin* gene transcription was obviously initiated very quickly after the isolation of HSC as documented in this study, since the mRNA of Nestin was already detectable at the first day of culture in the majority of cell preparations. The Nestin protein synthesis remained undetectable in quiescent HSC cultured for 1 day; although the *Nestin* DNA was not found to be methylated, another epigenetic mechanism for silencing of *Nestin* transcription was sought. It turned out that quiescent HSC apparently inhibited the *Nestin* expression by histone H3 methylation at lysine 9, an inhibitory methylation site. Culture-activated HSC, in contrast, may enhance *Nestin* transcription through histone H3 methylation at lysine 4. The same inhibitory epigenetic mechanism of *Nestin* expression via histone H3 methylation of lysine 9 as documented for HSC was found in ESC of rats. The level of histone H3 methylation at lysine 9 was substantially higher in ESC than in HSC and indicates that the onset of *Nestin* gene transcription already started in some stellate cells shortly after their isolation. This might explain the detection of Nestin mRNA in many primary cultures of HSC at day 1. However, a similar regulation of *Nestin* expression via histone modification was recently observed in other undifferentiated cells. It was reported, that the *Nestin* DNA methylation is not sufficient to regulate Nestin expression in teratocarcinoma cells and neural stem cells [40]. Regarding to the BS sequencing results of HSC, umbilical cord blood stem cells, and ESC, the findings reported in [40] were confirmed, because no *Nestin* DNA methylation was detected in these cells. However, in differentiated cells such as hepatocytes and also in the hepatoma cell line H4IIE the *Nestin* DNA was methylated. The DNA methylation was shown to control *Nestin* expression in H4IIE cells, since the demethylation by Aza treatment led to an induction of Nestin. These findings represent the first description of a cell type-dependent regulation of *Nestin* expression via DNA methylation. Taken together, the results of the epigenetic regulation of *Nestin* lead to the hypothesis that this factor is differentially regulated in undifferentiated and differentiated cells. One may speculate that the histone modification is more easy reversible than the DNA methylation, and, as a result of this, it might facilitate rapid Nestin expression when stem cell activation is required.

Owing to the fact that Nestin expression is well documented for culture-activated HSC [20] and also indicates stem/progenitor cells that apparently preserved their developmental potential, this protein was used in the present study as a marker to analyze stellate cell activation after liver injury in vivo. In 2 models of liver injury (PH and PH in the presence of AAF) the analysis of Nestin by Western blot, immunofluorescence, and qRT-PCR clearly showed a stellate cell activation during liver regeneration. The expression of α-SMA was also found to be transiently upregulated as investigated by Western blot and immunofluorescence stainings, whereas an increased deposition of collagen type I as a hallmark of fibrosis remained undetectable [41]. The Nestin expression was even more pronounced in the liver after application of AAF followed by PH. This is in good agreement with the general view that this model is able to induce a stem cell response. Cytokines such as tumor necrosis factor α and interleukin-6, which are known to influence liver regeneration, failed to affect the Nestin expression of cultured HSC (not shown). Nestin is rather required for cell migration and metastasis as demonstrated for prostate cancer cells [42].

Nestin-positive activated HSC, as identified by co-staining with desmin, were found to be located on cytokeratin 19-expressing cells as a part of the ductular reaction during liver regeneration after PH in the presence of AAF. In this model, duct-like structures appeared around the seventh day after PH. Although liver progenitor cells termed "oval cells" were reported to express Nestin [43], the simultaneous detection of Nestin and cytokeratins, as classical "oval cell" markers, displayed distinct immunofluorescence stainings in the portal field (Fig. 5D), indicating that the HSC mainly contributed to the elevated *Nestin* expression during liver regeneration. After PH without AAF, when hepatocyte proliferation mainly contributes to the restoration of liver mass, HSC were also activated as indicated by their *Nestin* expression. A remodeling of their niche in the space of Dissé [19] through the proliferation of adjacent hepatocytes at the first day after PH may account for their activation, since cell–cell contacts between HSC and hepatocytes were most likely disturbed. A rapid reconstitution of the liver tissue could be one reason for the early decline of *Nestin* expression in this model of liver injury. Although the exact contribution of stellate cells to liver regeneration remains to be elucidated, the analysis of Nestin clearly indicated an early stellate cell activation in both models of liver injury.

Acknowledgments

The authors are grateful to Claudia Rupprecht for expert technical assistance. This study was supported by Deutsche Forschungsgemeinschaft through Collaborative Research Center SFB 575 "Experimental Hepatology," Düsseldorf.

Author Disclosure Statement

No competing financial interests exist.

References

1. Riggs AD and TN Porter. (1996). Overview of genetic mechanisms. In: *Epigenetic Mechanisms of Gene Regulation.* Russo

VEA, RA Martienssen, AD Riggs, eds. Cold Spring Harbor Laboratory Press, Cold Spring Harbor, NY, pp 29–45.
2. Riggs AD. (1975). X-inactivation, differentiation and DNA methylation. Cytogenet Cell Genet 14:9–25.
3. Clark-Adams CD, D Norris, MA Osley, JS Fassler and F Winston. (1988). Changes in histone gene dosage alter transcription in yeast. Genes Dev 2:150–159.
4. Verdel A, S Jia, S Gerber, T Sugiyama, S Gygi, SI Grewal and D Moazed. (2004). RNAi-mediated targeting of heterochromatin by the RITS complex. Science 303:672–676.
5. Jahner D, H Stuhlmann, CL Stewart, K Harbers, J Lohler, I Simon and R Jaenisch. (1982). *De novo* methylation and expression of retroviral genomes during mouse embryogenesis. Nature 298:623–628.
6. Holliday R and JE Pugh. (1975). DNA modification mechanisms and gene activity during development. Science 187: 226–232.
7. Bestor TH and VM Ingram. (1983). Two DNA methyltransferases from murine erythroleukemia cells: purification, sequence specificity, and mode of interaction with DNA. Proc Natl Acad Sci USA 80:5559–5563.
8. Li E, TH Bestor and R Jaenisch. (1992). Targeted mutation of DNA methyltransferase gene results in embryonic lethality. Cell 69:915–926.
9. Okano M, DW Bell, DA Haber and E Li. (1999). DNA methyltransferases Dnmt3a and Dnmt3b are essential for *de novo* methylation and mammalian development. Cell 99: 247–257.
10. Li E, C Beard and R Jaenisch. (1993). Role for DNA methylation in genomic imprinting. Nature 366:362–365.
11. Little M and B Wainwright. (1995). Methylation and p16: suppressing the suppressor. Nat Med 7:633–634.
12. Klein WM, BP Wu, S Zhao, H Wu, AJ Klein-Szanto and SR Tahan. (2007). Increased expression of stem cell markers in malignant melanoma. Mod Pathol 20:102–107.
13. Tabu K, K Sasai, T Kimura, L Wang, E Aoyanagi, S Kohsaka, M Tanino, H Nishihara and S Tanaka. (2008). Promoter hypomethylation regulates CD133 expression in human gliomas. Cell Res 18:1037–1046.
14. Baba T, PA Convery, N Matsumura, RS Whitaker, E Kondoh, T Perry, Z Huang, RC Bentley, S Mori, S Fujii, JR Marks, A Berchuck and SK Murphy. (2009). Epigenetic regulation of CD133 and tumorigenicity of $CD133^+$ ovarian cancer cells. Oncogene 28:209–218.
15. Sen GL, JA Reuter, DE Webster, L Zhu and PA Khavari. (2010). DNMT1 maintains progenitor function in self-renewing somatic tissue. Nature 463:563–567.
16. Kordes C, I Sawitza, A Müller-Marbach, N Ale-Agha, V Keitel, H Klonowski-Stumpe and D Häussinger. (2007). $CD133^+$ hepatic stellate cells are progenitor cells. Biochem Biophys Res Commun 352:410–417.
17. Jackson M, A Krassowska, N Gilbert, T Chevassut, L Forrester, J Ansell and B Ramsahoye. (2004). Severe global DNA hypomethylation blocks differentiation and induces histone hyperacetylation in embryonic stem cells. Mol Cell Biol 20:8862–8871.
18. Gard A, F White and G Dutton. (1985). Extra-neural glial fibrillary acidic protein (GFAP) immunoreactivity in perisinusoidal stellate cells of rat liver. J Neuroimmunol 8:359–375.
19. Sawitza I, C Kordes, S Reister and D Häussinger. (2009). The niche of stellate cells within rat liver. Hepatology 50:1617–1624.
20. Niki T, M Pekny, K Hellemans, P De Bleser, K Van Den Berg, F Vaeyens, E Quartier, F Schutt and A Geerts. (1999). Class VI intermediate filament protein nestin is induced during activation of rat hepatic stellate cells. Hepatology 29:520–527.
21. Wiese C, A Rolletschek, G Kania, P Blyszczuk, KV Tarasov, Y Tarasova, RP Wersto, KR Boheler and AM Wobus. (2004). Nestin Expression—a property of multi-lineage progenitor cells? Cell Mol Life Sci 61:2510–2522.
22. Tatematsu M, RH Ho, T Kaku, JK Ekem and E Farber. (1984). Studies on the proliferation and fate of oval cells in the liver of rats treated with 2-acetylaminofluorene and partial hepatectomy. Am J Pathol 114:418–430.
23. Mann J, F Oakley, F Akiboye, A Elsharkawy, AW Thorne and DA Mann. (2007). Regulation of myofibroblast transdifferentiation by DNA methylation and MeCP2: implications for wound healing and fibrogenesis. Cell Death Differ 14:275–285.
24. Mann J, DC Chu, A Maxwell, F Oakley, NL Zhu, H Tsukamoto and DA Mann. (2010). MeCP2 controls an epigenetic pathway that promotes myofibroblast transdifferentiation and fibrosis. Gastroenterology 138:705–714.
25. Kordes C, I Sawitza and D Häussinger. (2009). Hepatic and pancreatic stellate cells in focus. Biol Chem 390:1003–1012.
26. Nyfeler Y, RD Kirch, N Mantei, DP Leone, F Radtke, U Suter and V Tayler. (2005). Jagged1 signals in the postnatal subventricular zone are required for neural stem cell self-renewal. EMBO J 24:3504–3515.
27. Karanu FN, L Yuefei, L Gallacher, S Sakano and M Bhatia. (2003). Differential response of primitive human $CD34^-$ and $CD34^+$ hematopoetic cells to the Notch ligand Jagged-1. Leukemia 17:1366–1374.
28. Hendriks HFJ, WA Verhoofstad, A Brouwer, AM DeLeeuw and DL Knook. (1985). Perisinusoidal fat-storing cells are the main vitamin A storage sites in rat liver. Exp Cell Res 160: 138–149.
29. Berry MN and DS Friend. (1969). High-yield preparation of isolated rat liver parenchymal cells. A biochemical and fine structural study. J Cell Biol 43:506–520.
30. Knook DL and EC Sleyster. (1976). Separation of Kupffer and endothelial cells of the rat liver by centrifugal elutriation. Exp Cell Res 99:444–449.
31. Higgins GM and RM Anderson. (1931). Experimental pathology of the liver. I. Restoration of the liver of the white rat following partial surgical removal. Arch Pathol Lab Med 12:186–202.
32. Pfaffl MW. (2001). A new mathematical model for relative quantification in real-time RT–PCR. Nucleic Acid Res 29: 2003–2007.
33. Dignam JD, RM Lebovitz and RG Roederer. (1983). Accurate transcription initiation by RNA polymerase II in a soluble extract from isolated mammalian nuclei. Nucleic Acid Res 11:1475–1489.
34. Bradford MM. (1976). A rapid and sensitive method for the quantitation of microgram quantities of protein utilizing the principle of protein-dye binding. Ann Biochem 7: 248–254.
35. Li LC and R Dahiya. (2002). MethPrimer: designing Primers for methylation PCRs. Bioinformatics 18:1427–1431.
36. Yang L, A Jung, A Omenetti, RP Witek, SS Choi, HM Vandongen, J Huang, GD Alpini and AM Diehl. (2008). Fate-mapping evidence that hepatic stellate cells are epithelial progenitors in adult mouse livers. Stem Cells 26:2104–2113.
37. Kordes C, I Sawitza and D Häussinger. (2008). Canonical Wnt signaling maintains the quiescent stage of hepatic stellate cells. Biochem Biophys Res Commun 367:116–123.

38. Takenobu H, O Shimozato, T Nakamura, H Ochiai, Y Yamaguchi, M Ohira, A Nakagawara and T Kamijo. (2011). CD133 suppresses neuroblastoma cell differentiation via signal pathway modification. Oncogene 30:97–105.
39. Walker L, M Lynch, S Silverman, J Fraser, J Boulter, G Weinmaster and JC Gasson. (1999). The Notch/Jagged pathway inhibits proliferation of human hematopoietic progenitors in vitro. Stem Cells 17:162–171.
40. Han DW, JT Do, MJ Araúzo-Bravo, SH Lee, A Meissner, HT Lee, R Jaenisch and HR Schöler. (2009). Epigenetic hierarchy governing nestin expression. Stem Cells 27:1088–1097.
41. Kordes C, I Sawitza and D Häussinger. (2011). Stellate cells in the regenerating liver. In: *Liver Regeneration.* Häussinger D, ed. De Gruyter, Berlin. www.degruyter.de/cont/fb/na/detail.cfm?id=IS-9783110250787-1
42. Kleeberger W, GS Bova, ME Nielsen, M Herawi, AY Chuang, JI Epstein and DM Berman. (2007). Roles for the stem cell associated intermediate filament Nestin in prostate cancer migration and metastasis. Cancer Res 67:9199–9206.
43. Gleiberman AS, JM Encinas, JL Mignone, T Michurina, MG Rosenfeld and G Enikolopov. (2005). Expression of nestin-green fluorescent protein transgene marks oval cells in the adult liver. Dev Dyn 234:413–421.

Address correspondence to:
Dr. Claus Kordes
Klinik für Gastroenterologie, Hepatologie und Infektiologie
Heinrich-Heine-Universität
Moorenstraße 5
40225 Düsseldorf
Germany

E-mail: claus.kordes@t-online.de

Dr. Dieter Häussinger
Klinik für Gastroenterologie, Hepatologie und Infektiologie
Heinrich-Heine-Universität
Moorenstraße 5
40225 Düsseldorf
Germany

E-mail: haeussin@uni-duesseldorf.de

Received for publication September 22, 2010
Accepted after revision January 10, 2011
Prepublished on Liebert Instant Online January 10, 2011